diagnostics

MDPI

*Article*

# Automatic analysis of ultrasound images to estimate subcutaneous, visceral fat and muscle tissue in patients with suspected malnutrition

**Antonio Cuesta-Vargas [1,2]*, José María Arjona-Caballero [1,2], Gabriel Olveira [2,3,4,5], Daniel de Luis Román [6,7], Diego Bellido Guerrero [8] and Manuel García-Almeida [2,3]**

[1]Clinimetria Research Group, Department of Physiotherapy, Faculty of Health Sciences, Universidad de Malaga, 29071 Malaga, Spain; acuesta@uma.es
[2]Institute of Biomedical Research in Malaga (IBIMA-Bionand Platform), 29590 Málaga, Spain
[3] Department of Endocrinology and Nutrition, Hospital Regional Universitario de Málaga, Málaga, Spain. gabolvfus@uma.es jgarciaalmeida@gmail.com
[4]Department of Medicine and Dermatology. Faculty of Medicine, University of Malaga, Malaga, Spain
[5]Centro de Investigación Biomédica en Red (CIBER) de Diabetes y Enfermedades Metabólicas Asociadas, Instituto de Salud Carlos III, Málaga, Spain
[6] Endocrinology and Nutrition Department, Clinical University Hospital of Valladolid, 47003 Valladolid, Spain; dluisro@saludcastillayleon.es
[7] Investigation Centre Endocrinology and Nutrition, Faculty of Medicine, University of Valladolid, 47003 Valladolid, Spain
[8]Department of Endocrinology and Nutrition, Complejo Hospitalario Universitario de Ferrol (CHUF), 15405 Ferrol, A Coruna, Spain; diegobellido@gmail.com
* Correspondence: acuesta@uma.es

**Abstract:** Malnutrition is a prevalent condition associated with adverse health outcomes, requiring accurate assessment of muscle composition and fat distribution. This study presents a novel method for the automatic analysis of ultrasound images to estimate subcutaneous and visceral fat, as well as muscle, in patients with suspected malnutrition. The proposed system utilizes computer vision techniques to segment regions of interest (ROI), calculate relevant variables, and store data for clinical evaluation. A dataset of abdominal and leg ultrasound images, captured in both longitudinal and transversal planes, was analyzed. Results showed higher precision for longitudinal scans compared to transversal scans, particularly for length-related variables, with the Y-axis Vastus intermediate achieving a precision of 92.87%. However, area-based measurements demonstrated lower precision due to differences between manual adjustments by experts and automatic geometric approximations. These findings highlight the system's potential for clinical use while emphasizing the need for further algorithmic refinements to improve precision in area calculations.

**Keywords:** ULTRASOUND IMAGING; MUSCLE COMPOSITION; MALNUTRITION; IMAGE SEGMENTATION; COMPUTER VISION; CLINICAL DIAGNOSTICS

## 1. Introduction

Body composition is a fundamental aspect in determining an individual's health status, influenced by environmental, genetic, and lifestyle factors[1]. Health professionals utilize body composition assessment as an essential tool to measure their patients' nutritional status and to identify and diagnose conditions such as overweight, obesity, malnutrition, osteoporosis, and sarcopenic obesity [2]

From the perspective of diagnosing and treating nutrition-related diseases, the identification and measurement of fat, muscle, bone, and water are critical. Therefore, body

composition evaluation is a crucial element, involving the separation of an individual's total mass into fat mass and fat-free mass, where fat-free mass includes muscles, organs, ligaments, tendons, and water [3].

Ultrasound has established itself as a fundamental tool in clinical medicine due to its ability to evaluate body tissues and structures. This non-invasive, portable, cost-effective, real-time technique that does not emit ionizing radiation offers multiple advantages [4], although it presents the challenge of accurately interpreting the obtained data. Musculoskeletal ultrasound is a technique that uses high frequencies to obtain detailed images of skeletal muscle [6], allowing the observation of hierarchical relationships of soft tissues and their internal structures, as well as extracting characteristics such as muscle texture and echogenicity.

The analysis of these ultrasound images provides important clinical variables such as muscle thickness, the area of subcutaneous fat zones, and other variables directly related to the patient's health status. These variables allow a precise evaluation of the evolution of certain pathologies. Through ultrasound, it is possible to obtain relevant information from variables such as thickness, echo intensity, echo variation, grey-level co-occurrence matrices, and echo texture parameters. These variables have been described in both healthy individuals and those with various diseases [7], [8], [9].

Accurately quantifying both muscle and fat tissue status is essential for assessing a patient's health status. There is a growing interest in using ultrasound as a tool for body composition analysis, especially concerning sarcopenia [8]. Although several studies have suggested its potential, more research is still needed to validate its use in different populations [7], [10]. Particularly, in malnourished patients, there is a shortage of studies evaluating body composition estimation using ultrasound images. Using ultrasound for body composition evaluation in this population could be promising, as it is a non-invasive and low-cost technique [11]. Identifying new biomarkers from ultrasound images could help in the early detection and monitoring of malnutrition and its complications, thereby improving the care and treatment of these patients [12].

The analysis of ultrasound images is a laborious process due to the presence of noise and the geometric complexity of the structures. Typically, this analysis requires a specialist to manually select the area of interest using interactive software, which can lead to errors, especially in patients with complex body structures. Moreover, this manual method is not suitable for analyzing large batches of serial images. For these reasons, an automated analysis method is necessary, allowing specialists to accurately obtain the variables of interest, thus improving diagnoses.

Various methods have been proposed to measure structural parameters through ultrasound images, especially muscle parameters. For instance, the MUSA method, proposed by Caresio and Salvi et al. [13], automates the measurement of muscle thickness in ultrasound images by detecting muscle fascicles using the Hough transform and an iterative heuristic search to identify aponeurosis contours and calculate muscle thickness. However, noise and the presence of blood vessels can hinder accuracy, and the method only measures muscle thickness. To address these limitations, TRAMA [14] was developed, using the Sobel operator and a Gaussian filter to segment cross-sectional ultrasound images of muscles, improving the identification of aponeuroses.

Zheng et al. proposed an automated method based on segmentation with Residual Shrinkage-Unet [15], achieving precise and comprehensive measurement of muscle parameters by eliminating complex noise. On the other hand, Burlina et al. [16] explored the automatic diagnosis of myositis using deep neural networks, achieving an accuracy of 79.2%. Marzola et al. [17] developed a method for diagnosing abnormal muscles based on the grey level of the cross-sectional area, achieving a classification accuracy of 91.5%. Zhou et al. [18] implemented a multitasking model, MMA-Net, for segmenting the cross-sectional muscle area and classifying abnormal muscles, achieving very high performance.

In general, the aforementioned automatic methods present several problems [15]; they are typically not fully automatic, relying on manual selection of filters or areas of

interest and are often highly sensitive to images with significant noise or the presence of unusual shapes.

In this article, we propose a method for the automatic analysis of ultrasound images based on computer vision. This system automatically segments the area of interest and analyzes the segmented image to automatically extract the clinical variables of interest. This automated analysis method can reduce the diagnostic burden on physicians and provide an effective basis for subsequent treatment. The method is based on the use of computer vision and predefined ultrasound zone templates to automatically detect areas of interest.

## 2. Materials and Methods

In this article, we propose a method for the automatic analysis of ultrasound images aimed at estimating muscle composition in patients with suspected malnutrition using computer vision techniques.

### *2.1. Data*

A large volume of anonymized images was compiled from two areas (abdomen and-leg) and two planes (transverse and longitudinal). These images were captured using a commercially available portable ultrasound system with a 4–10 cm linear tube (UProbe L6C Ultrasound Scanner, Guangzhou Sonostar Technologies Co., Ltd., Guangzhou, China). From March to December 2022, consecutive patients aged 18 to 85 years admitted to the medical-surgical departments of the participating hospitals (excluding intensive care units [ICUs]) were eligible for inclusion if they were identified as being at risk of malnutrition during the first week of hospitalization and had provided informed consent.

All images were obtained from patients at collaborating hospitals [22,23], with ethical approval from the relevant committees. The study protocol was approved by the Ethics Committee for Clinical Research (CEIC) of the Health Council of the Andalusian Health Service (protocol code ALM-DRECO-2021-01, approval date 1 February 2022) and the individual Institutional Review Boards of the participating hospitals. Written informed consent was obtained from all patients.

Image Acquisition Procedure

The following procedure was followed for image acquisition: For the leg images, the patient lay down and the structure was located using the upper edge of the patella and the anterior superior iliac spine. The transducer was placed 14 cm above the patella, centered on the thigh. For transverse scans, the transducer was positioned perpendicular to the muscle fibers, and for longitudinal scans, it was rotated to align with the fibers once the tendon was located.

For the abdominal images, the patient also lay down and the midpoint between the xiphoid process and the navel was located. The transducer was placed transversely to the muscle fibers and then rotated to the longitudinal position.

### *2.2. Data Analysis and Processing*

Once the images are obtained, the Open CV system proceeds with their analysis and processing. An Open CV system refers to a framework or software solution built using OpenCV (Open-Source Computer Vision Library), which provides tools and algorithms for real-time computer vision and image processing. The primary objective of this system is to segment the image into specific regions, calculate the region of interest (ROI), and extract relevant features. Once extracted, the images are automatically stored in a database for subsequent consultation by clinical staff.

The images are uploaded to the system, allowing for the analysis of both individual images and batches. The system supports the inclusion of images in. dcm, .jpg, .bmp, and .png formats. The image processing involves the following stages:

Image Segmentation

Using a predefined code in the image notation, specific areas for segmentation are identified. The image is divided into four main regions: Lateral Leg, Transverse Leg, Lateral Abdomen, and Transverse Abdomen. This segmentation is crucial as it allows subsequent algorithm stages to focus on specific areas of the image, enhancing the accuracy and relevance of the analysis.

Image Correction

Once segmented, the image undergoes an initial correction process. This process prepares the image for further analysis through color conversion and scale adjustments.

Conversion to RGB: The initially loaded image is converted to RGB format to ensure a standard color representation.

Conversion to Grayscale: Subsequently, the RGB image is converted to grayscale. This conversion simplifies subsequent processing by reducing the amount of information to be handled, focusing solely on pixel intensity.

Calculation of the Region of Interest (ROI)

The region of interest (ROI) is a specific section of the image containing the relevant data for analysis. The ROI calculation is performed using a threshold-based approach on horizontal and vertical axes.

Horizontal Thresholds: The region on the x-axis containing relevant data is determined. This is done by moving from a central position to the left and right, calculating the mean of the data from the central point to the extremes. If the mean falls below a preset threshold, that point is defined as the endpoint of the ROI on the x-axis.

Vertical Thresholds: Using the previously cropped image with horizontal thresholds, the region on the y-axis containing relevant data is determined. This is done by moving from a central position upwards and downwards, subsequently calculating the mean of the data as in the previous case.

Image Filtering

The next step of the algorithm is filtering the image to remove noise and improve data quality. A bilateral filter is used to remove noise while preserving edges. A bilateral filter with a standard deviation for the range distance of 5 and a standard deviation for the color set at 0.1 is applied.

Image Normalization

Finally, the filtered image is normalized to ensure consistent representation and facilitate subsequent calculations. The image is converted to a range of values between 0 and 255.

Template Matching and Contour Detection

After normalization, template matching and contour detection are performed to identify and delineate the structures present in the image.

For contour detection, the binarized image of the ROI is used. This process utilizes the open-source package OpenCV version 4.8.074 in Python 3.10. Subsequently, the detected contours are compared with predefined templates for each area. These templates have been previously annotated and extracted from images analyzed by an expert professional. Template matching is performed using the match Template method, with template matching correlation as the comparison method.

To enhance system performance, specific constraints are applied. Template detection is performed in both directions: from the lower position (deepest muscle) to the upper position (skin) and from the upper position to the lower position. The detection process ensures that each template is identified within its designated range, considering the

relative positions between templates. For each match found, the corresponding contour is extracted. This approach allows for precise identification and delineation of the structures within each region of interest while ensuring consistency across both search directions. The following figure 1 shows the delimited zones detected using the templates.

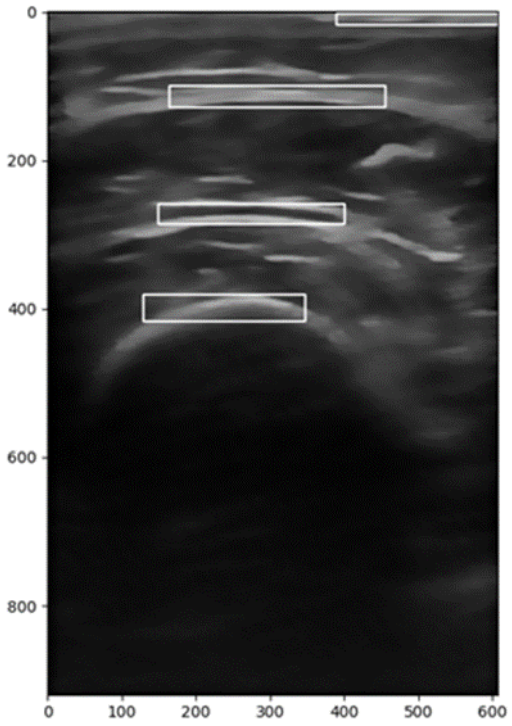



**Figure 1.** Zones detected corresponding to the templates.

Calculation of Distances and Areas

With the positions of the detected contours, the algorithm proceeds to calculate the relevant distances and areas. Distances between different zones of interest, such as the distance between muscles and skin, are calculated. This involves calculating the distance between the edges of the contours to determine the height. The width is the width of the image, which was previously defined during the initial processing.

Once the height and width of the zone are determined, the area is calculated using rectangular and elliptical approximations, depending on the shape of the zone. For elliptical areas, the direct least squares method [23] is used to fit the ellipse shape to the image shape.

Feature Extraction

Finally, the algorithm extracts various variables of interest from the obtained data and the initial image

### *2.3. Variables of Interest*

In this article, various ultrasound variables have been extracted and classified into two main categories: length and area variables, and image characteristic variables.

Length and Area Variables

The study includes four types of images: transverse abdomen, longitudinal abdomen, transverse leg, and longitudinal leg. Length and area variables allow for the quantification of physical dimensions within the images. Table 1 includes the variables depending on the area and cut.

**Table 1.** Length and area variables according to cut and zone.

| | **Abdomen** | **Leg** |
|---|---|---|
| Longitudinal | Total Subcutaneous Fat<br>Superficial Subcutaneous Fat<br>Peritoneal Fat | Y-axis Anterior Rectus<br>X-axis Anterior Rectus<br>Anterior Rectus Area<br>Y-axis Vastus Intermedius<br>X-axis Vastus Intermedius<br>Vastus Intermedius Area |
| Transverse | Total Subcutaneous Fat<br>Superficial Subcutaneous Fat<br>Peritoneal Fat | Y-axis Anterior Rectus<br>X-axis Anterior Rectus<br>Anterior Rectus Area<br>Y-axis Vastus Intermedius<br>X-axis Vastus Intermedius<br>Vastus Intermedius Area |

Image Characteristic Variables

In addition to the length and area variables, various image characteristic variables were analyzed for all the mentioned types of images. These variables are based on the textural and statistical properties of the ultrasound images:

- Angular Second Moment (ASM): Also known as uniformity or energy, this measure evaluates the repetition and uniformity of gray levels. A high ASM value indicates greater uniformity.
- Contrast: Measures the variation in gray levels between neighboring pixels. High contrast indicates a clear distinction between light and dark areas.
- Correlation: Assesses the linear dependence between the gray levels of pixels in a specific direction. A value of 0 indicates no correlation.
- Dissimilarity: Measures the difference between the gray levels of adjacent pixels. A high value reflects greater variability.
- Entropy: Used to evaluate the lack of uniformity in the image texture. Higher entropy indicates lower uniformity.
- Histogram: Represents the normalized distribution of gray levels in the image, providing the mean of these levels.
- Homogeneity: Indicates the similarity between the gray levels of the pixels in the image, being a measure of textural uniformity.

### *2.4. Data Storage*

The calculated values of the characteristics are returned and stored in a database for further analysis and use in research or medical diagnostics.

Interface

Once the data is in the database, the end user can query and download all extracted variables through a web interface designed for this purpose. Users can query individual patients or groups based on hospital, visits, regions, cuts, etc.

### *2.4. Statistical Methods*

The Bland–Altman analysis method was employed to evaluate the agreement between two measurement techniques. This approach uses a scatter plot to display the differences between the two methods against their mean, offering a clear view of the agreement, bias, and limits of agreement. Statistical analysis and calculations were conducted using RStudio 2023.06.0 Build 421 (Posit Software, PBC, formerly RStudio, PBC. The open-source data science company, located at 250 Northern Ave, Suite 420, Boston, MA, USA 02210, 844-448-1212)

## 3. Results

The analysis of ultrasound muscle segmentation for subcutaneous and visceral fat, as well as muscle characteristics, yielded the following results. Table 2 summarizes the adjusted precision percentages for each evaluated variable. The variables were compared with manual analysis performed by an expert operator using a modified version of the application that allows for area selection.

For the abdominal region, subcutaneous fat measurements showed higher precision in longitudinal scans compared to transversal ones, with subcutaneous fat total reaching 71.42% and subcutaneous fat superficial at 68.77%. Precision for peritoneal fat was slightly lower, reaching 63.00%. Transversal cuts in the abdominal region demonstrated consistently lower precision, particularly for subcutaneous fat superficial, which reached 55.65%.

In the leg region, both longitudinal and transversal scans demonstrated variability in precision. For longitudinal cuts, the Y-axis Rectus femoris achieved a precision of 80.43%, while the precision for the Rectus femoris area was significantly lower at 43.29%. Similarly, for transversal cuts, the intermediate area of the Vastus reached only 41.05%, while the Y-axis Vastus intermediate exceeded expectations with a precision of 92.87%.

Overall, area analyses show lower precision compared to manual calculations. However, areas such as the Rectus femoris area and subcutaneous fat superficial demonstrated room for improvement, suggesting potential algorithmic refinement or dataset adjustments. The figure 2.1 (longitudinal section) and figure 2.2 (transverse section) shown the agreement between two measurements techniques.

**Table 2.** Accuracy of the analysis.

| Member | Section | Type | Accuracy |
|---|---|---|---|
| Abdomen | Longitudinal | Subcutaneous fat total | 71.42 |
| | | Subcutaneous fat superficial | 68.77 |
| | | Peritoneal fat | 63.0 |
| | Transversal | Subcutaneous fat total | 54.3 |
| | | Subcutaneous fat superficial | 55.65 |
| | | Peritoneal fat | 51.02 |
| Leg | Transversal | Y-axis Rectus femoris | 78.73 |
| | | Rectus femoris area | 28.09 |
| | | Y-axis Vastus intermediate | 81.65 |
| | | Vastus intermediate area | 43.31 |
| | Longitudinal | Subcutaneous fat | 40.82 |
| | | Y-axis Rectus femoris | 83.85 |
| | | Rectus femoris area | 46.33 |
| | | Y-axis Vastus intermediate | 81.39 |
| | | Vastus intermediate area | 36.52 |

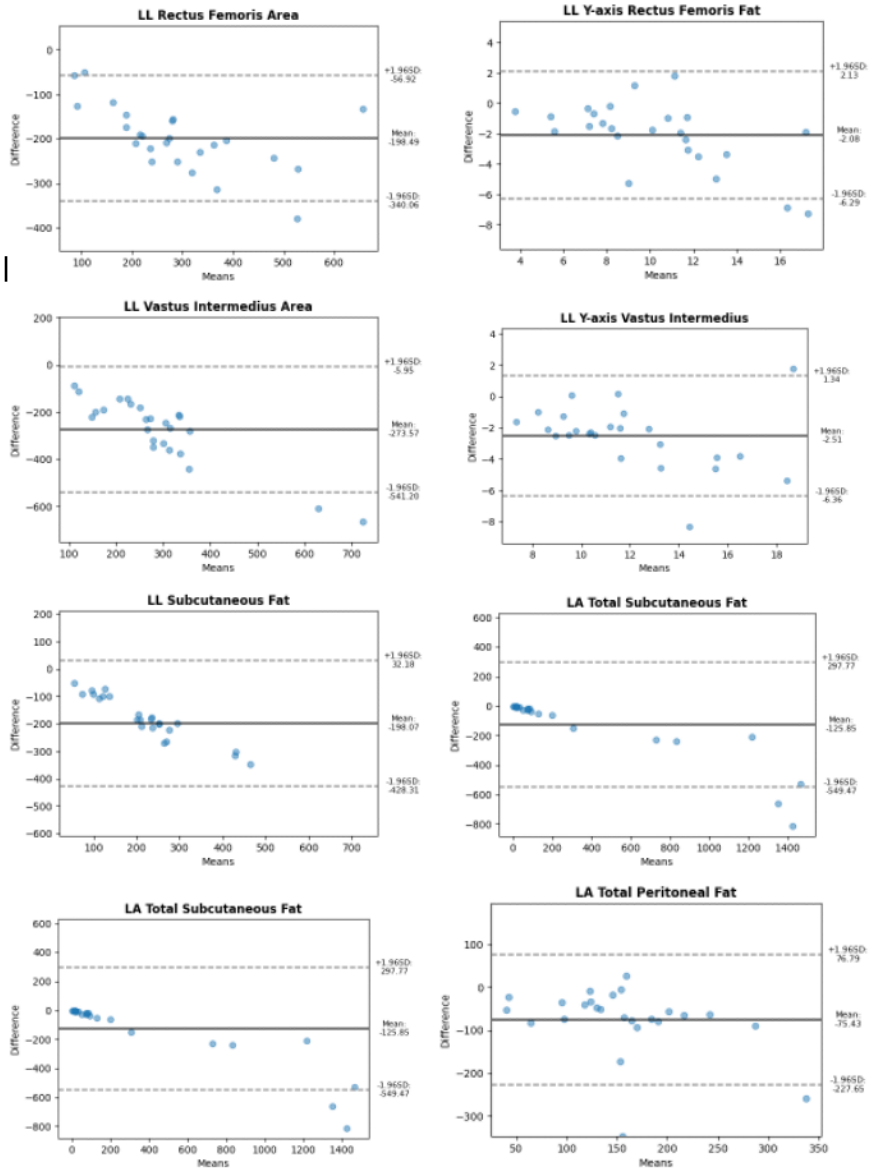



**Figure 2.1 Bland-Altman Plot Longitudinal muscle, subcutaneous and visceral fat tissues**

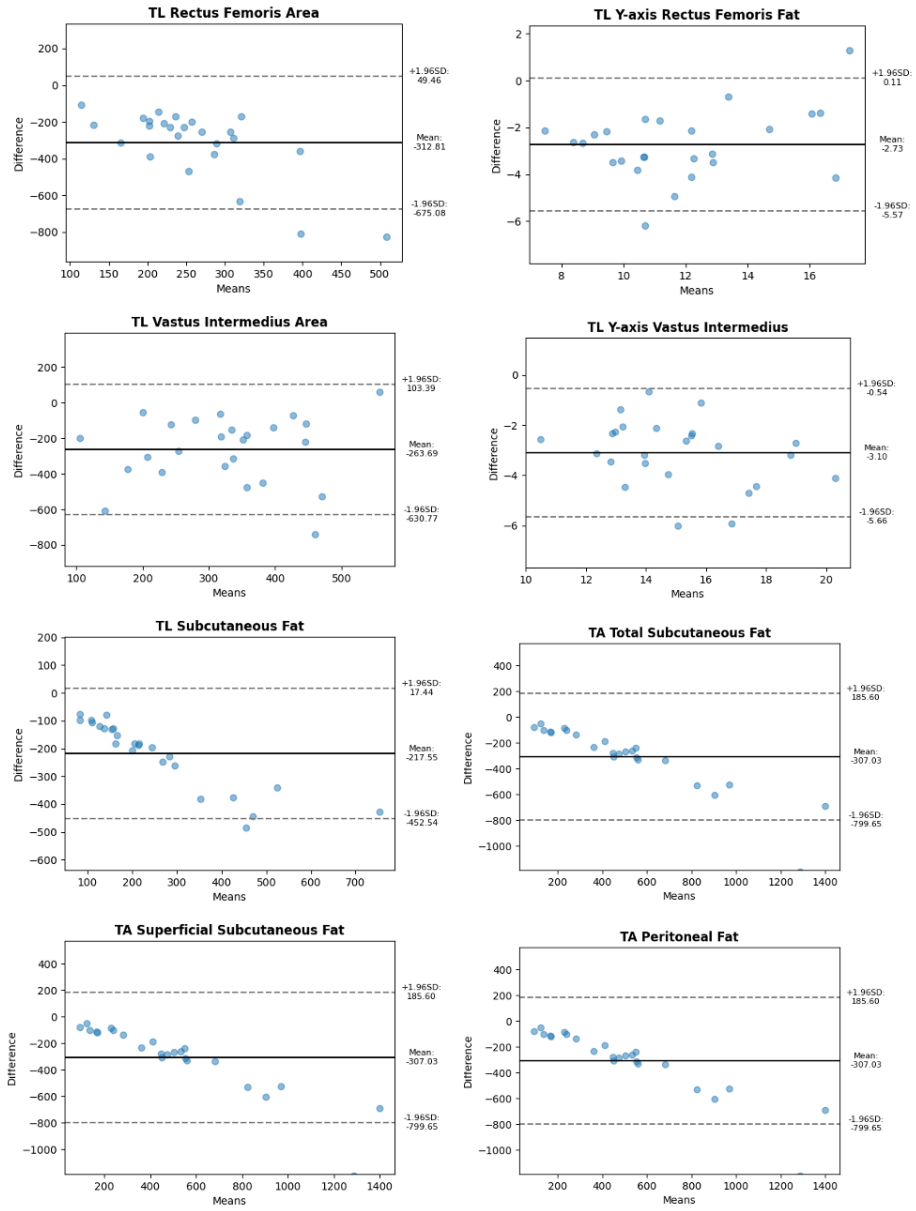



**Figure 2.2 Bland-Altman Plot Transverse (axial) muscle, subcutaneous and visceral fat tissues**

## 4. Discussion

The proposed method for the automatic analysis of ultrasound images successfully segmented muscle structures and estimated fat composition in patients with suspected malnutrition. The results demonstrate that longitudinal scans generally provide higher precision compared to transversal scans, particularly in measuring subcutaneous fat and muscle axes. For example, the Y-axis Vastus intermediate in the leg region achieved the highest precision of 92.87%, while other variables such as Rectus femoris area and subcutaneous fat superficial showed significant room for improvement.

One key observation is the consistent discrepancy in precision for area calculations when compared to manual analysis performed by expert operators. This can be attributed to the differences in measurement approaches: manual analysis allows precise adjustment of areas, while the automatic method approximates the shapes to geometric figures, such as rectangles or ellipses. These approximations inherently introduce variability and limit the precision of the algorithm in delineating complex anatomical regions. This study underscores the importance of incorporating expert-annotated datasets and exploring hybrid approaches that combine manual and automated analysis to bridge the gap in precision and ensure the method's clinical applicability.

Despite these limitations, the system demonstrated its potential as a reliable tool for estimating relevant variables in ultrasound images, particularly for length-related measures. First, it was conducted exclusively in patients with malnutrition associated with disease, limiting its generalizability to this specific population. Second, while ultrasound (US) is not widely utilized for assessing muscle mass in patients with disease-related malnutrition (DRM), clinical guidelines recommend its use, and a recent study demonstrated good accuracy of this automatic methods based on IA analysis [24]. Third, the study focused on a single muscle, the rectus femoris. Lastly, the automated method used requires replication and cross-validation with another cohort and comparison against MRI/CT. Despite these limitations, the study has notable strengths: the ultrasound imaging of the RF was meticulously standardized.

Future work should focus on refining the segmentation and shape-fitting algorithms to reduce discrepancies in area calculations. Additionally, increasing the diversity and quality of the training dataset could enhance the system's robustness across different patient profiles and ultrasound devices.

## 5. Conclusions

In this report, an automated method for the analysis of ultrasound images was developed to estimate muscle composition in patients with suspected malnutrition. The approach leverages computer vision techniques to automatically segment regions of interest and extract clinically relevant variables, reducing manual workload and improving diagnostic accuracy. The system processes images through stages of segmentation, correction, filtering, normalization, and contour detection, utilizing OpenCV and bilateral filtering. Key variables, including thickness and texture features, are extracted and stored in a database for clinical use. Despite challenges with noisy or low-quality images, the method shows promise for enhancing the assessment of body composition, particularly in malnourished patients. Future research will focus on improving robustness by use of advanced neural networks and the automatic detection of the area and type of scan to eliminate the need for file annotation.

**Author Contributions:** For research articles with several authors, a short paragraph specifying their individual contributions must be provided. The following statements should be used "Conceptualization, AC-V; methodology, AC-V.; software, AC-V.; validation, AC-V.; formal analysis, AC-V; investigation, AC-V ;resources, AC-V; data curation AC-V ; writing—original draft preparation, AC-V writing—review and editing AC-V; G.O; MG-A; DL-R; DB-G visualization, AC-V ,supervision, AC-V; G.O; MG-A; DL-R; DB-G; project administration, AC-V.; funding acquisition, AC-V; G.O; MG-A; DL-R; DB-G. All authors have read and agreed to the published version of the manuscript.".

**Funding:** This research was funded in part by Abbott Laboratories, but the founding source has no role in the design of the study, analysis, interpretation of data, or decisions regarding the publication of results.

**Institutional Review Board Statement:** The study protocol was approved by the Ethics Committee for Clinical Research (CEIC) of the Health Council of the Andalusian Health Service (protocol code ALM-DRECO-2021-01, approval date 1 February 2022) and the individual Institutional Review Boards of the participating hospitals.

**Informed Consent Statement:** Informed consent was obtained from all subjects involved in this study.

**Data Availability Statement:** Data are unavailable due to privacy and ethical restrictions.

**Acknowledgments:** We thank K ACCESS Health & Abbott S.L. for providing administrative and technical support, for assistance in the use equipment, and for comments on the manuscript.

**Conflicts of Interest:** The remaining authors declare that the research was conducted in the absence of any commercial or financial relationships that could be construed as a potential conflict of interest.

## References

1. Holmes CJ, Racette SB. The Utility of Body Composition Assessment in Nutrition and Clinical Practice: An Overview of Current Methodology. Nutrients. 2021;13:2493.

2. García-Almeida JM, García-García C, Vegas-Aguilar IM, Ballesteros Pomar MD, Cornejo-Pareja IM, Fernández Medina B, de Luis Román DA, Bellido Guerrero D, Bretón Lesmes I, Tinahones Madueño· FJ. Nutritional ultrasound®: Conceptualisation, technical considerations and standardisation Endocrinología, Diabetes y Nutrición 70 (2023) S74---S84

3. Cederholm T, Jensen GL, Correia MITD, Gonzalez MC, Fukushima R, Higashiguchi T, Baptista G, Barazzoni R, Blaauw R, Coats A, Crivelli A, Evans DC, Gramlich L, Fuchs-Tarlovsky V, Keller H, Llido L, Malone A, Mogensen KM, Morley JE, Muscaritoli M, Nyulasi I, Pirlich M, Pisprasert V, de van der Schueren MAE, Siltharm S, Singer P, Tappenden K, Velasco N, Waitzberg D, Yamwong P, Yu J, Van Gossum A, Compher C; GLIM Core Leadership Committee; GLIM Working Group. GLIM criteria for the diagnosis of malnutrition - A consensus report from the global clinical nutrition community. Clin Nutr. 2019 Feb;38(1):1-9. doi: 10.1016/j.clnu.2018.08.002. Epub 2018 Sep 3. PMID: 30181091.

4. Bazzocchi A, Filonzi G, Ponti F, Albisinni U, Guglielmi G, Battista G. Ultrasound: Which role in body composition? Eur J Radiol. 2016;85:1469–80.

5. García-Almeida JM, García-García C, Ballesteros-Pomar MD, Olveira G, Lopez-Gomez JJ, Bellido V, Bretón Lesmes I, Burgos R, Sanz-Paris A, Matia-Martin P, et al. Expert Consensus on Morphofunctional Assessment in Disease-Related Malnutrition. Grade Review and Delphi Study. *Nutrients*. 2023; 15(3):612. https://doi.org/10.3390/nu15030612

6. Ozçakar L, Tok F, De Muynck M, Vanderstraeten G. Musculoskeletal ultrasonography in physical and rehabilitation medicine. J Rehabil Med. 2012;44:310–8.

7. Escriche-Escuder A, Trinidad-Fernández M, Pajares B, Iglesias-Campos M, Alba E, García-Almeida JM, et al. Responsiveness of the new index muscular echotexture in women with metastatic breast cancer: an exercise intervention study. Sci Rep. 2022;12:15148.

8. Kawai H, Kera T, Hirayama R, Hirano H, Fujiwara Y, Ihara K, et al. Morphological and qualitative characteristics of the quadriceps muscle of community-dwelling older adults based on ultrasound imaging: classification using latent class analysis. Aging Clin Exp Res. 2018;30:283–91.

9. Ríos-Díaz J, Del Baño-Aledo ME, Tembl-Ferrairó JI, Chumillas MJ, Vázquez-Costa JF, Martínez-Payá JJ. Quantitative neuromuscular ultrasound analysis as biomarkers in amyotrophic lateral sclerosis. Eur Radiol. 2019;29:4266–75.

10. Escriche-Escuder A, Trinidad-Fernández M, Pajares B, Iglesias-Campos M, Alba E, Cuesta-Vargas AI, et al. Ultrasound use in metastatic breast cancer to measure body composition changes following an exercise intervention. Sci Rep. 2021;11:8858.

11. Guirado-Peláez P, Fernández-Jiménez R, Sánchez-Torralvo FJ, Mucarzel Suárez-Arana F, Palmas-Candia FX, Vegas-Aguilar I, Amaya-Campos MdM, Martínez Tamés G, Soria-Utrilla V, Tinahones-Madueño F, et al. Multiparametric Approach to the Colorectal Cancer Phenotypes Integrating Morphofunctional Assessment and Computer Tomography. *Cancers*. 2024; 16(20):3493. https://doi.org/10.3390/cancers16203493

12. de Luis Roman D, García Almeida JM, Bellido Guerrero D, Guzmán Rolo G, Martín A, Primo Martín D, García-Delgado Y, Guirado-Peláez P, Palmas F, Tejera Pérez C, et al. Ultrasound Cut-Off Values for Rectus Femoris for Detecting Sarcopenia in Patients with Nutritional Risk. *Nutrients*. 2024; 16(11):1552. https://doi.org/10.3390/nu16111552

13. Caresio C, Salvi M, Molinari F, Meiburger KM, Minetto MA. Fully Automated Muscle Ultrasound Analysis (MUSA): Robust and Accurate Muscle Thickness Measurement. Ultrasound Med Biol. 2017;43:195–205.

14. Salvi M, Caresio C, Meiburger KM, De Santi B, Molinari F, Minetto MA. Transverse Muscle Ultrasound Analysis (TRAMA): Robust and Accurate Segmentation of Muscle Cross-Sectional Area. Ultrasound Med Biol. 2019;45:672–83.

15. Zheng W, Zhou L, Chai Q, Xu J, Liu S. Fully Automatic Analysis of Muscle B-Mode Ultrasound Images Based on the Deep Residual Shrinkage U-Net. Electronics. 2022;11:1093.

16. Burlina P, Billings S, Joshi N, Albayda J. Automated diagnosis of myositis from muscle ultrasound: Exploring the use of machine learning and deep learning methods. PloS One. 2017;12:e0184059.

17. Marzola F, van Alfen N, Doorduin J, Meiburger KM. Deep learning segmentation of transverse musculoskeletal ultrasound images for neuromuscular disease assessment. Comput Biol Med. 2021;135:104623.

19. Zhou L, Liu S, Zheng W. Automatic Analysis of Transverse Musculoskeletal Ultrasound Images Based on the Multi-Task Learning Model. Entropy Basel Switz. 2023;25:662.

20. Ritsche P, Franchi MV, Faude O, Finni T, Seynnes O, Cronin NJ. Fully Automated Analysis of Muscle Architecture from B-Mode Ultrasound Images with DL_Track_US. Ultrasound Med Biol. 2024 Feb;50(2):258-267. doi: 10.1016/j.ultrasmedbio.2023.10.011. Epub 2023 Nov 25. PMID: 38007322.

21. García Almeida JM, Bellido D, De Luis D, Guzmán Rolo G, Olveira G. Protocol for a prospective cohort study on the feasibility of application of nutritional ultrasound in the diagnosis and follow-up of patients with nutritional risk at hospital discharge: study on body composition and function (DRECO). BMJ Open. 2023 Dec 9;13(12):e074945. doi: 10.1136/bmjopen-2023-074945. PMID: 38070895; PMCID: PMC10729227.

22. García Almeida JM, Bellido D, De Luis D, et alProtocol for a prospective cohort study on the feasibility of application of nutritional ultrasound in the diagnosis and follow-up of patients with nutritional risk at hospital discharge: study on body composition and function (DRECO)BMJ Open 2023;13:e074945. doi: 10.1136/bmjopen-2023-074945

23. Fitzgibbon A, Pilu M, Fisher RB. Direct least square fitting of ellipses. IEEE Trans Pattern Anal Mach Intell. 1999;21:476–80.

24. García-Herreros S, López Gómez JJ, Cebria A, Izaola O, Salvador Coloma P, Nozal S, Cano J, Primo D, Godoy EJ, de Luis D. Validation of an Artificial Intelligence-Based Ultrasound Imaging System for Quantifying Muscle Architecture Parameters of the Rectus Femoris in Disease-Related Malnutrition (DRM). Nutrients. 2024 Jun 8;16(12):1806. doi: 10.3390/nu16121806. PMID: 38931161; PMCID: PMC11206908.

**Disclaimer/Publisher's Note:** The statements, opinions and data contained in all publications are solely those of the individual author(s) and contributor(s) and not of MDPI and/or the editor(s). MDPI and/or the editor(s) disclaim responsibility for any injury to people or property resulting from any ideas, methods, instructions or products referred to in the content.